Spatial distribution of atoms in a magneto-optical trap

V. S. Bagnato, L. G. Marcassa, M. Oria, G. I. Surdutovich, R. Vitlina, and S. C. Zilio
Instituto de Física e Química de São Carlos, Universidade de São Paulo,
Caixa Postal 369, 13560-970 São Carlos, São Paulo, Brazil
(Received 2 April 1993)

We present a theoretical analysis to explain the origin of different spatial distributions of laser-cooled sodium atoms in a magneto-optical trap. Such distributions, which include spherical clouds, rings, and rings with cores, are attributed to the radiation pressure due to misaligned Gaussian beams acting on each individual atom. The predictions of this theory are confirmed by experimental observations reported earlier. We were able to construct a diagram with several domains corresponding to the stable structures observed.

PACS number(s): 32.80.Pj, 42.50.Vk

I. INTRODUCTION

Trapping and cooling of neutral atoms are important techniques that have recently been studied both theoretically and experimentally. The most efficient trap for neutral atoms is the magneto-optical trap [1] (MOT) based on the spontaneous radiation pressure acting on the atomic system in the presence of an inhomogeneous magnetic field. The use of the MOT has allowed a great advance in studies of cold collisions [2–5], high-resolution spectroscopy [6,7], nonlinear optics [8], and fundamental aspects of laser cooling. A good understanding of the dynamics of trapped atoms may help in the achievement of higher densities and lower temperatures.

Experiments carried out recently have demonstrated that different spatial distributions of atoms such as stable rings and rings with central cores are possible in MOT's [9–11]. We investigate here the changes in the spatial distribution of atoms in a MOT caused by variations of the trap conditions such as laser intensity, detuning, misalignment, and magnetic-field gradient. Such changes seem to be similar to phase transitions. This work was motivated by two recent experiments [11,12] where, in opposition to previous results [9], it was observed that in some situations ring-shaped distributions of atoms in MOT's are independent on the number of trapped atoms. We have employed the concept of a coordinate-dependent vortex force acting on a two-level atom to justify the observed structures and to create a "phase diagram" showing several domains of trapping conditions where different spatial distributions are stable. Experimental observations reported earlier [11], and partially reproduced here as illustration, strongly support the present model.

II. EXPERIMENTAL APPARATUS

In our experiments we employ a MOT formed by the intersection of three orthogonal laser beams which are retroreflected after passing through a sodium cell. The trap is loaded from the vapor in a cell heated to about 60 ° C, consisting of a stainless-steel chamber with several windows allowing the entrance of the trapping beams and the visual observation. The image of the trap is recorded by a commercial charge-coupled device (CCD) television camera. The laser beams, derived from a Coherent 699 ring dye laser, passes through a homemade electro-optical (EO) modulator. The modulator produces frequency sidebands at 1712 MHz, one of which works as a repumper for atoms that decay to the ground not resonant with the trapping frequency $[3S_{1/2}(F=2) \rightarrow 3P_{3/2}(F=3)]$. The beam from the EO modulator is split in three arms and passes through quarter-wave plates producing circular polarized light, which are introduced into the cell. Before retroreflecting, each beam passes through a second quarter-wave plate which ensures that the two counter-propagating beams have opposite circular polarizations. The magnetic field is produced by a pair of parallel coils carrying opposite currents. This configuration produces an axial field gradient up to 25 G/cm and a transverse field gradient of half of the axial one.

Atoms in the MOT are subject to radiative forces with velocity and magnetic-field dependences [1]. The velocity dependence is usually referred to as the damping force and since by assumption the atoms are already cold, we will consider only the first-order approximation for this force. The trapping force comes from the dependence of the photon scattering rate on the magnetic-field gradient and in the harmonic approximation only the term $(dB/dx)x$ is kept. The MOT is similar to a damped harmonic oscillator.

III. OBSERVATION OF DIFFERENT SPATIAL DISTRIBUTIONS OF ATOMS

With the laser beams well retroreflected and crossing at $B=0$, we observe a cloud of trapped atoms of about 1 mm in diameter at the center of the trap for all detunings where the trap works. Under such conditions, the spatial atomic distribution is close to spherical. On the other hand, when the laser beams are slightly misaligned [as shown in Fig. 1(a)] different spatial distributions, mainly contained in the xy plane, are observed. At a high field gradient (typically 25 G/cm) and/or small misalignment (typical displacement of about $0.2w$ where w is half of the

Gaussian beam waist) we observe a cloud of atoms close to the trap minimum with minor distortions [Fig. 1(b)]. However, as the misalignment increases, different structures are observed depending on the detuning, laser intensity, and field gradient. For large detunings ($|\Delta| \sim 2\Gamma$, where Γ is the transition linewidth and for sodium $\Gamma/2\pi = 10$ MHz), moderate field gradients (typically $dB/dx = 10$ G/cm) and moderate laser intensities ($I/I_s = 1$ to 2 per beam, where I_s is the saturation intensity), we found that for beam displacements s between 0.5 and 2 (in units of half-waist w) the atoms are distributed in a ring-shaped structure, as shown in Fig. 1(c). This kind of structure has already been observed for different atoms as reported in Refs. [9–11]. However, smaller values of detunings and higher powers produce a different structure where a core of atoms, as shown in Fig. 1(d). This last structure (ring with a central core) appears to be not as stable as the others. Sudden jumps taking this distribution to a ball of atoms or sometimes to a ring have been observed. This instability increases considerably if vibrations of the mirrors or fluctuations in the magnetic field are present, which leads us to believe that such instability is caused by mechanical instabilities of the system.

IV. A MODEL BASED ON A COORDINATE-DEPENDENT VORTEX FORCE

In order to explain our results we have developed a model based on a radiative vortex force [11]. In the present work, this concept is extended in a way to generate a phase diagram which can predict the spatial structure for a given set of experimental parameters. Consider the trapping laser beams configuration as shown in Fig. 1(a) for the xy plane and the z direction beam perfectly retroreflected. We will consider all beams as ideal Gaussian functions, such that the Rabi frequency for each one can be written as $\Omega = \Omega_0 \exp(-r^2/2w^2)$. Due to the misalignment, the radiative force acting on the atom along the y direction has an x dependence and vice versa. Besides the velocity- and field-dependent terms in the force expression, there is an extra component which is referred to as the vortex force.

Let us consider the force acting on an atom placed along the x axis. The results obtained in this case can be extended to anywhere in the plane through a convenient rotation if the atom is close to the trap center such that the trap anisotropy can be neglected. The presence of the

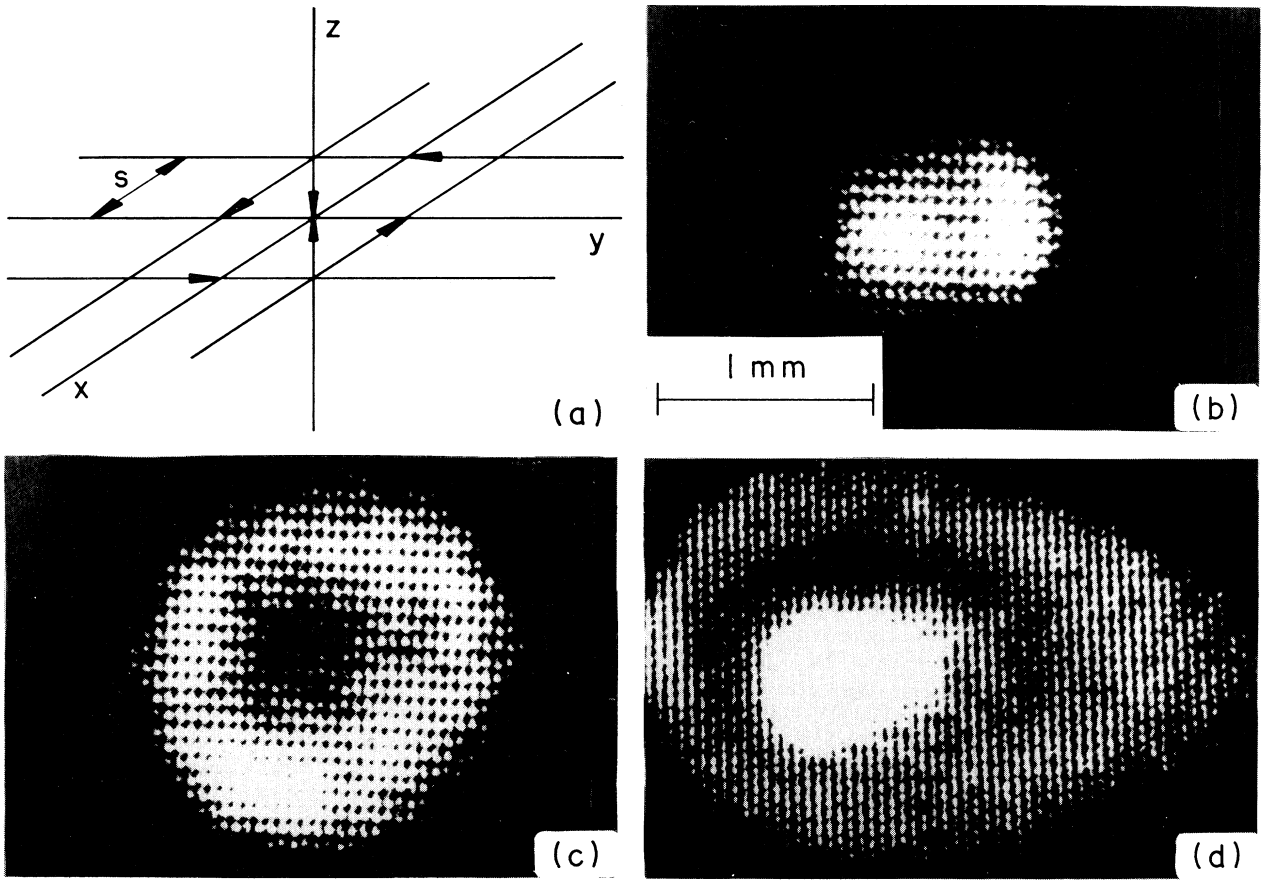

FIG. 1. (a) Geometry of the laser beams forming a racetrack in the xy plane and aligned in the z direction. The displacement of each beam is labeled s. (b) Atomic distribution for small misalignment and/or high field gradient. (c) Moderated misalignment and field gradient. (d) Same as in (c), but with higher laser intensity and smaller detuning.

vortex force produces a torque on the atoms and induces a rotation around the trap center. For the geometry considered here the velocity is mainly in the y direction. There are small x components of the vortex and damping forces which are not important for our analysis. The total force acting on the atom is, in units of $\hbar k\Gamma$ ($\hbar$ is Planck's constant and k the inverse of the radiation wavelength)

$$\mathbf{f}=-Kx\hat{\mathbf{x}}-\alpha v\hat{\mathbf{y}}+F(x)\hat{\mathbf{y}} , \tag{1}$$

where v is the velocity and the trapping constant (K) is

$$\frac{K}{2\pi}=\frac{16\Omega_0^2|\Delta|}{(1+2\Omega_0^2)^2\left[1+\dfrac{4\Delta^2}{1+2\Omega_0^2}\right]^2}\frac{d\omega}{dx} , \tag{2}$$

where Δ is the laser detuning and $d\omega/dx$ is the variation of the transition frequency with position due to the inhomogeneous field. The damping constant α is

$$\frac{\alpha}{2\pi}=\frac{16|\Delta|\Omega_0^2(k/\Gamma)}{(1+2\Omega_0^2)^2\left[1+\dfrac{4\Delta^2}{1+2\Omega_0^2}\right]^2} , \tag{3}$$

with k/Γ being the ratio between the wave number of the radiation and the transition linewidth. For simplicity we have considered all frequencies in units of Γ and distances in units of w. Equations (2) and (3) assume an atom with a $J=0$ ground state and a $J=1$ excited state. Finally,

$$F(x)=\frac{be^{-x^2+2xs}}{1+2be^{-x^2+2xs}}-\frac{be^{-x^2-2xs}}{1+2be^{-x^2-2xs}} , \tag{4}$$

with $b=\Omega_0^2\exp(-s^2)/(4\Delta^2+1)$, is the vortex force arising from the misalignment of the Gaussian laser beams. An atom in this configuration is accelerated by the vortex force until its velocity becomes large enough so that the vortex force is balanced by the damping force. The energy removed by the damping is replaced by the work of the vortex force. This situation may produce a stable circular trajectory. Assuming the conditions $\alpha v=F(x)$ and $mv^2/x=Kx$ (m is the atomic mass), one finds

$$\alpha\sqrt{K/m}\,x=F(x) . \tag{5}$$

The first term $[\alpha(K/m)^{1/2}x]$, called the "effective trapping force," has the effect of pulling the atom towards the trap center. In order to analyze the consequences of condition (5) on the atomic distribution in the trap, let us consider Fig. 2(a), where we have plotted $F(x)$ and the effective trapping force as a function of x. From Fig. 2(a) one can see the existence of two distinct cases: In case (a.I), $\alpha(K/m)^{1/2}>F'(0)$ [first derivative of $F(x)$ at $x=0$], in which the only point where Eq. (5) holds is at $x=0$. In this case the effective trapping force is always larger than the vortex force, pulling the atoms towards the trap center. The only possible stable distribution of atoms for this case is a ball of atoms around the origin. In case (a.II), $\alpha(K/m)^{1/2}<F'(0)$, where Eq. (5) is fulfilled at $x=0$ and x_0. However, $x=0$ does not correspond to a stable solution because at that point the vortex

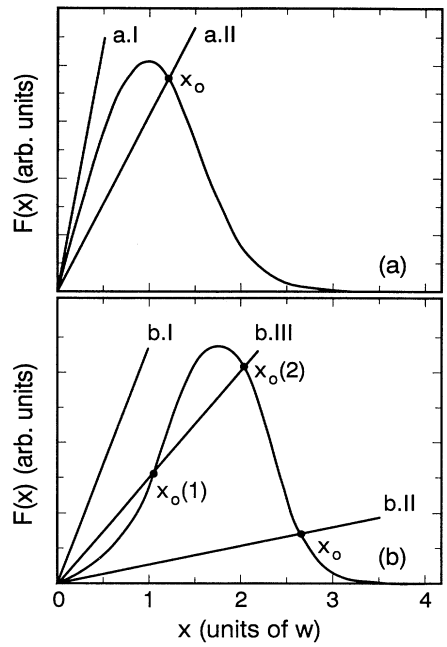

FIG. 2. (a) Graphical representation of Eq. (5) when moderate misalignment and laser intensity are employed. (b) Typical graphical representation of Eq. (5) for high laser intensity and/or large misalignment.

(which is always trying to force the atoms to spiral out of the origin) is larger than the effective trapping force and atoms cannot stay at that point. They move out until they get to the point $x=x_0$, which now represents a stable point because for $x<x_0$ the vortex force is larger and dominates, pulling the atom back to x_0, and for $x>x_0$ the effective trapping force is larger pushing the atom back to x_0. Thus $x=x_0$ represents a stable position for the atoms and the structure in this case corresponds to a ring.

The shape of the vortex force in Fig. 2(a) only holds for moderate power and misalignment. If the laser power is well above saturation or if a large misalignment is used, instead of having $F''(0)<0$ [second derivative of $F(x)$ at $x=0$], one has $F''(0)>0$, which corresponds to a change in the concavity of the vortex force, which under these conditions takes the shape of Fig. 2(b). In this situation we have three possible cases where Eq. (5) is satisfied: case (b.I) is similar to case (a.I) with the stable structure in the trap being a bell of atoms (close to the center). Case (b.II) is similar to case (a.II) (however, in this case the ring may be too large for our approximation to be valid). Finally, case (b.III) corresponds to have $\alpha(K/m)^{1/2}>F'$ (with $F''>0$). The last condition (b.III) will present three points where Eq. (5) can be satisfied. At $x=0$, the effective trapping force is larger than the vortex force, hence this is a stable point and atoms can stay there. At $x_0(1)$ the equilibrium is unstable since atoms located at $x<x_0(1)$ will be pulled to $x=0$ because the effective trapping force is larger and atoms at $x>x_0(1)$ will be pushed towards $x_0(2)$, which corre-

sponds to a stable point. At any given time an atom must necessarily be at only one point of stability. However, for an ensemble of atoms there can be atoms at both stable points. As a result, in case (b.III), atoms can be at the center of the trap or circulating in a ring of radius close to $x_0(2)$ and in such case a ring of atoms with a central core can be observed. Summarizing this discussion, depending on the values of laser intensity, detuning, magnetic-field gradient, and misalignment, it is possible to find the three structures presented in Fig. 1. Starting from a conventional trap configuration (no misalignment) we experimentally observe a sudden jump to a ring as s is increased such that the condition $F'(0) > \alpha(K/m)^{1/2}$ is fulfilled.

We have performed a numerical simulation of the atomic motion in the presence of six Gaussian beams. Simulations corresponding to the conditions where the three structures of Fig. 1 were observed are shown in Fig. 3. In Fig. 3(a) we have the simulated atomic trajectory for conditions of small misalignment and low laser intensity (specific values of all parameters are given in the figure caption). For these parameters, any atom, no matter what the initial condition, always ends at the trap center. Keeping the same parameters, except for the misalignment, which is now increased, we observe that the atomic trajectories always evolve to a ring-shaped structure, as shown in Fig. 3(b). For this case we have simulated two different trajectories starting at different points and both end at the same stable ring trajectory. Increasing considerably the laser intensity [Fig. 3(c)], the stable points now depend on the initial conditions. Atoms that start close to the center will end at the center. However, atoms which start far from the center will end in a stable ring. The final configuration for atoms with several initial conditions will be a ring with a central core as experimentally observed and shown in Fig. 1(d).

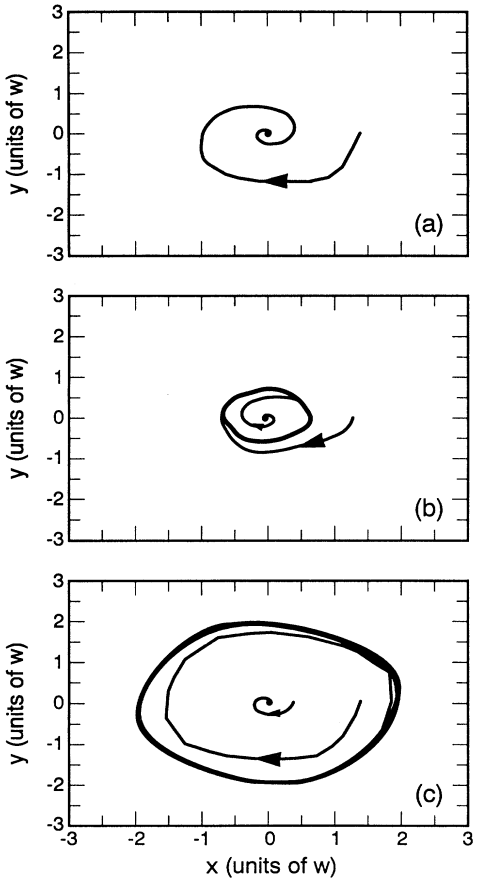

FIG. 3. Computer-simulated atomic trajectories for the three main observed structures (distances in units of w and frequencies are in units of Γ). (a) $s=1.0$, $\Delta=-2.5$, $d\omega/dx=1$, $\Omega_0=4$; (b) $s=2.2$, $\Delta=-2.5$, $d\omega/dx=1$, $\Omega_0=4$; and (c) $s=1.2$, $\Delta=-2.5$, $d\omega/dx=1$, $\Omega_0=12$.

Although we have found that the stable structures for the trapped atoms is very dependent on the several parameters involved, for some range of values of intensity and misalignment only two structures seem to appear. For example, for very small misalignment the only stable structure is a ball of atoms at the trap center independent on how large the laser intensity, detuning, and field gradient are.

V. A DIAGRAM FOR THE STABLE STRUCTURES

Considering expressions (4) and (5) we have analytically worked out under what conditions one should expect each of the described structures. As a result of these considerations, we have produced a diagram which has as coordinates the misalignment and the effective laser intensity [represented by the term $\Omega_0^2/(4\Delta^2+1)$]. Different regions of this diagram correspond to different domains of stable structures. We call this a "phase diagram" for atomic distributions in a magneto-optical trap. For $\Delta=-\Gamma$, the resultant diagram is presented in Fig. 4 as a full line. With the exception of the first region (left of line *ABC*), where only one structure is possible (ball of atoms), other domains always present two possible struc-

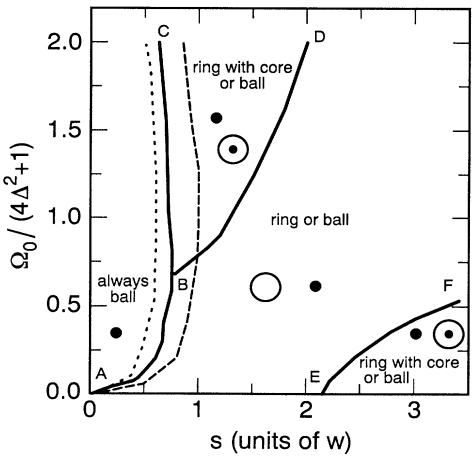

FIG. 4. Diagram showing different possibilities of spatial distributions of atoms depending on laser intensity and misalignment. The full line corresponds to $\Delta=-\Gamma$. Changing the laser detuning, the lines of the diagram shift and the sizes of the domains change. As an example we show the changes in one of the lines for different detunings: $\Delta=-0.7\Gamma$ (dashed line) and $\Delta=-1.2\Gamma$ (dotted line).

tures. The one that will actually be observed depends on the magnetic-field gradient used. As an example, in the domain corresponding to a ring or ball (right-hand side of line ABD) we will never observe a ring with core. However, higher dB/dx produces a ball of atoms while lower dB/dx produces a ring. Sometimes, jumps between the two possible structures are observed if the system is operating inside one of the domains but the magnetic field is close to the critical value. In fact, we have observed such a jumps in our experiment. Conditions close to the transition region between domains are very unstable and very sensitive to fluctuations in laser frequency, intensity, and alignment. We could produce very stable rings and balls of atoms, but due to limitations in our present experimental conditions stable and steady rings with core could not be observed. The ring with a core structure stays for about 1–2 sec. After that it jumps to another configuration, coming back to the original one on the same time scale. This means that we were near the transition line *BD*, which in Fig. 2(b) would correspond to condition (b.III), with $x_0(1)$ close to zero and $x_0(2)$ maximum. This is a condition very sensitive to fluctuations in the set up (mechanical, magnetic field, and frequency). To be deep inside the domain of ring plus core, we should have enough intensity to produce a normalized intensity of more than 1, even when working with detunings of the order of -2Γ. This constituted a limitation in the case of sodium such that we could only barely reach the domain of ring with core.

In the diagram of Fig. 4, the full line represents the case $\Delta=-\Gamma$. Shifts of the lines occur for different detunings, ass shown for $\Delta=-0.7\Gamma$ (dashed line) and $\Delta=-1.2\Gamma$ (dotted line). Each laser frequency will produce a diagram with different domain sizes.

Although we could not sweep through all conditions to experimentally determine the phase diagram, we have considered particular conditions where different structures should appear and indeed they were observed (Fig. 1). We have, however, performed computer simulations covering the entire plane of the phase diagram and numerically verified the existence of all structures.

We should point out that the diagram of Fig. 4 was obtained analytically in the approximation that the constants K and α do not have spatial dependence. A complete numerical calculation, including spatial variations of these constants, was carried out on the computer and the main features did not change. In this complete calculation we did not observe the domain for large displacement and low intensity, mainly because the trap does not work so well for such large displacement.

For the ring-shaped structure (without central core) we have performed a systematic study where the ring dimensions are measured as a function of several of the parameters involved. The independence of the number of atoms and the reasonable agreement of the dimensions strongly support the model presented here. Effects involving sub-Doppler cooling, as recently point out [13], seem to have little effect here; however, its degree of contribution remains to be studied.

VI. CONCLUSIONS

We have performed experimental observations only for sodium and the atomic densities that we have worked with range from 10^8 to 10^9 cm^{-3} (almost a factor of 1000 less than in previous work for cesium [9]). However, our model seems to apply to some extent for experiments involving cesium atoms as well as metastable neon [10]. Using the conditions reported for those two experiments, our model predicts well the observed structures and transitions. In the case of Ne*, their experimental conditions fall deep inside the region on the right-hand side of line ABD and only the ring structure is observed. On the other hand, for the Cs case they worked in the vicinity of the line *BC* and jumps between ring with core to ball of atoms were observed.

ACKNOWLEDGMENTS

This work is supported by Fundação de Amparo a Pesquisa do Estado de São Paulo. We are pleased to acknowledge K. Helmerson and W. Phillips for critical readings.

[1] E. Raab, M. Prentiss, A. Cable, S. Chu, and D. Pritchard, Phys. Rev. Lett. **59**, 2631 (1987).

[2] M. Prentiss, A. Cable, J. Bjorkholm, S. Chu, E. Raab, and D. Pritchard, Opt. Lett. **13**, 452 (1988).

[3] P. L. Gould, P.D. Lett, P. S. Julienne, W. Phillips, H. Thorsheim, and J. Weiner, Phys. Rev. Lett. **60**, 788 (1988).

[4] C. D. Wallace, T. P. Dinneen, K. Y. Tan, T. T. Grove, and P. L. Gould, Phys. Rev. Lett. **69**, 897 (1992).

[5] D. Sesko, T. Walker, C. Monroe, A. Gallagher, and C. Wieman, Phys. Rev. Lett. **63**, 961 (1989).

[6] D. Grison, B. Lounis, C. Salomon, J. Courtois, and G. Grynberg, Europhys. Lett. **15**, 149 (1991).

[7] M. Kasevich, E. Riis, S. Chu, and R. De Voe, Phys. Rev. Lett. **63**, 612 (1989).

[8] J. Tabosa, G. Chen, Z. Hu, R. Lee, and H. Kimble, Phys. Rev. Lett. **66**, 3245 (1991).

[9] T. Walker, D. Sesko, and C. Wieman, Phys. Rev. Lett. **64**, 408 (1990); D. Sesko, T. Walker, and C. Wieman, J. Opt. Soc. Am. B **8**, 946 (1991).

[10] F. Shimizu, K. Shimizu, and H. Takuma, in *Light Induced Kinetic Effects on Atoms, Ions and Molecules,* edited by L. Moi, S. Gozzini, C. Gabbanini, E. Arimondo, and F. Strumia (ETS Editrice, Pisa, 1991), p. 159.

[11] V. Bagnato, L. Marcassa, M. Oria, G. Surdutovich, and S. Zilio, Laser Phys. **2**, 172 (1992); see also T. Walker *et al.*, Phys. Lett. A **163**, 309 (1992).

[12] M. T. Araujo, V. S. Bagnato, G. I. Surdutovich, and S. C. Zilio (unpublished). We also learned recently that at AT&T Bell Laboratories, M. Prentiss and N. Bigelow observed rings in the MOT with dimensions that were independent of the number of atoms.

[13] A. Steane and C. Foot, Europhys. Lett. **14**, 231 (1991).

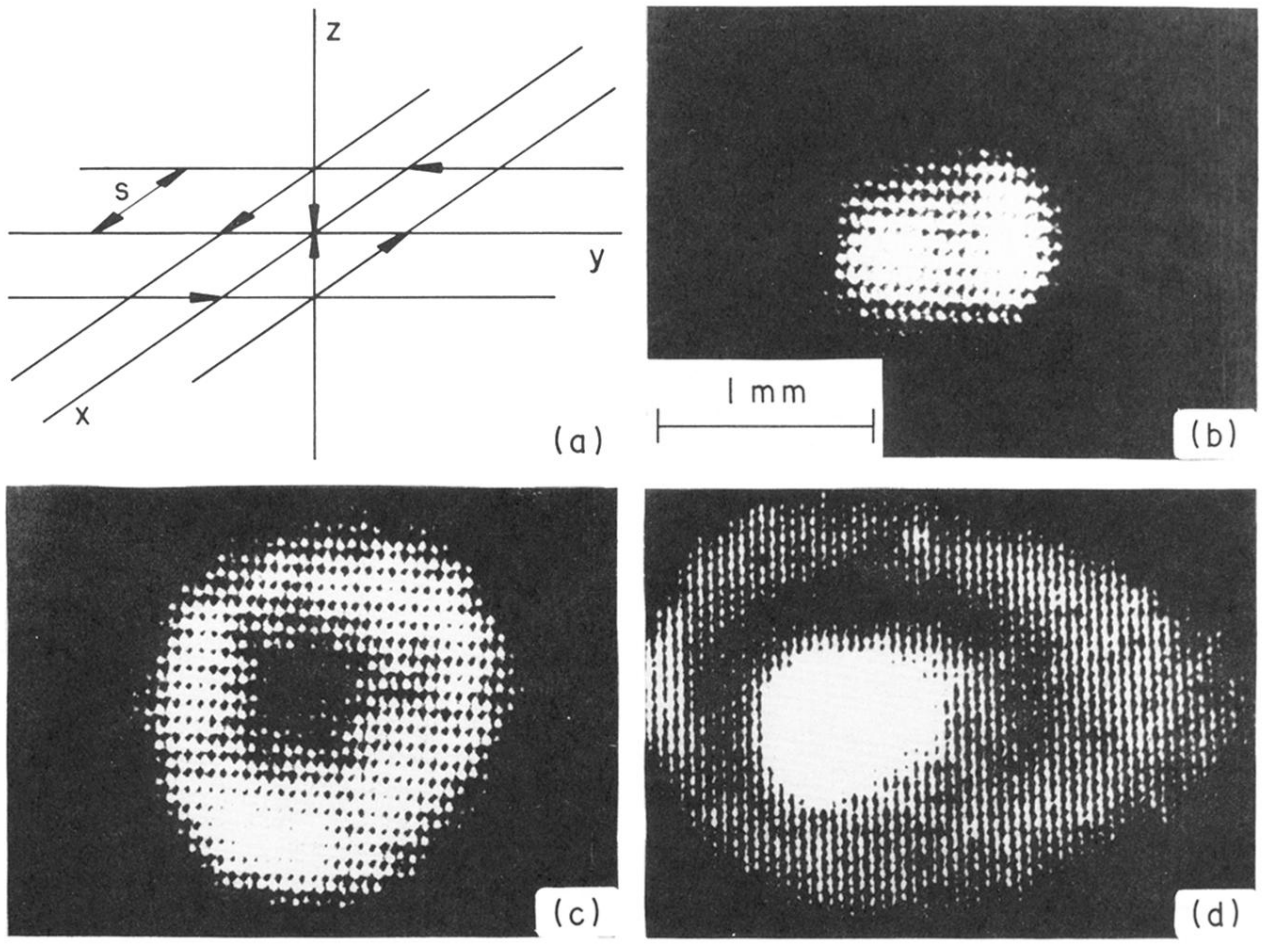

FIG. 1. (a) Geometry of the laser beams forming a racetrack in the xy plane and aligned in the z direction. The displacement of each beam is labeled s. (b) Atomic distribution for small misalignment and/or high field gradient. (c) Moderated misalignment and field gradient. (d) Same as in (c), but with higher laser intensity and smaller detuning.